APPLIED ORGANOMETALLIC CHEMISTRY
Appl. Organometal. Chem. 2006; **20**: 264–271
Materials, Nanoscience and Catalysis **AOC**
DOI:10.1002/aoc.1045

Polymerization of methyl methacrylate using bis(β-ketoamino)nickel(II)–MAO catalytic systems

Xiaohui He[1,2] and Qing Wu[1]*

[1]Institute of Polymer Science, School of Chemistry and Chemical Engineering, Zhongshan University, Guangzhou 510275, People's Republic of China
[2]Institute of Polymer Materials, Department of Material Science and Engineering, Nanchang University, Nanchang, Jiangxi 330029, People's Republic of China

Received 2 June 2005; Revised 22 December 2005; Accepted 22 December 2005

The polymerization of methyl methacrylate (MMA) was investigated using a series of bis(β-ketoamino)nickel(II) complexes in combination with methylaluminoxane in toluene solution. The binary catalyst is necessary for initiating MMA polymerization and producing PMMA with high molecular weights but broad molecular weight distributions. The effects of reaction temperature and Al : Ni molar ratios on the polymerization of MMA were examined in detail. Both steric bulk and electronic effects of the substituents around the imino group in the ligand on MMA polymerization activities could be observed. Relative to electronic effects, the steric hindrance of the ligands displayed a more significant effect on the catalytic activities, with the catalytic activity sequence observed in the order 4 > 1 > 2 > 3 > 5 > 6. Structural analyses of the polymers by ^{13}C NMR spectra indicate that polymerization yields PMMA with a syndiotactic-rich atactic microstructure. Copyright © 2006 John Wiley & Sons, Ltd.

KEYWORDS: late transition metal; methyl methacrylate; polymerization; syndiotacticity; catalysis

INTRODUCTION

To control the physical properties of polymer, such as toughness, adhesion, barrier properties, surface properties, miscibility with other polymers and rheological properties,[1] incorporating functional groups into nonpolar polymers is very important. However, simple coordination of the monomer functional group to the metal may block monomer access to vacant coordination sites, therefore functional monomer coordination insertion polymerization has become a challenging topic. Polar monomers, such as methyl methacrylate (MMA), are commonly polymerized though atom transfer radical and group transfer polymerization mechanisms catalyzed by selected metallocene catalysts such as $Cp^*_2LnR(Cp^* = \eta5\text{-}C_5(CH_3)_5$, Ln = Sm, Lu, Yb, R_2H or CH_3) and $(C_2H_4Ind)ZrMe_2/[Ph_3C][B(C_6F_5)_4]/Zn(C_2H_5)_2$, providing isotactic or syndiotactic PMMA based on the ligand structure.[2–5]

Late transition metal complexes are generally considered to be more tolerant toward polar media and polar functional groups due to their less oxophilic nature relative to early transition metal complexes, and make them likely targets for the development of catalysts for polar monomer polymerizations.[1,6] Nevertheless, there are still few reports on polar monomer coordination insertion polymerization catalyzed by late transition metal catalyst. Until recently, only a limited number of catalysts based on late transition metal have been used for homo- and copolymerization of polar monomers. Since the $Ni(acac)_2$–MAO catalyst system was first found to be an effective catalyst for the aspecific polymerization of MMA,[7–11] a great deal of attention has been directed to late-transition-metal-based complexes used as insertion-type polar monomer polymerization catalysts. Kim and co-workers reported that late transition metal complexes such as (α-diimine)nickel(II), (pyridyl bis-imine)iron(II) and (pyridyl bis-imine)cobalt(II), which are widely used for the polymerization of olefins,[6]

---

*Correspondence to: Qing Wu, Institute of Polymer Science, School of Chemistry and Chemical Engineering, Zhongshan University, Guangzhou 510275, People's Republic of China.
E-mail: ceswuq@zsu.edu.cn
Contract/grant sponsor: NSFC–SINOPEC; Contract/grant number: 20334030.
Contract/grant sponsor: Science Foundation of Guangdong Province; Contract/grant number: 039184.
Contract/grant sponsor: Ministry of Education of China; Contract/grant number: 20030558017.

will also polymerize polar monomers such as MMA in combination with methylaluminoxane (MAO) to give syndio-rich PMMA.[12,13]

In our previous work, we briefly reported that nickel (II) complexes bearing β-ketiminato ligands [N, O] could polymerize MMA to give syndio-rich PMMA with relatively wide molecular weight distributions after activation with MAO.[14] As a continuation of this study, we have synthesized and characterized a series of new bis(β-ketoamino)nickel(II) complexes by changing the steric bulk and electronic effects of the ligand, and investigated the effects of catalyst structure and polymerization conditions on the polymerization activity of methyl methacrylate using bis(β-ketoamino)nickel(II)–MAO as catalytic systems.

EXPERIMENTAL

Materials

All manipulations involving air- and moisture-sensitive compounds were performed under a dried and purified nitrogen atmosphere standard glove box and Schlenk techniques. Toluene was dried over sodium/benzophenone and distilled under nitrogen prior to use. Other solvents were purified using standard procedures. MMA, in which the inhibitor had been removed by washing twice with aqueous sodium hydroxide (5 wt%) and twice with water, was dried over anhydrous $MgSO_4$ and distilled over CaH_2 under N_2 atmosphere at reduced pressure (42 °C/70 mmHg), then dissolved in toluene to make a 0.5 g/ml solution. MAO was prepared by the hydrolysis of trimethylaluminum (TMA) with $Al_2(SO_4)_3 18H_2O$ in toluene; the initial $[H_2O]$:[TMA] molar ratio was 1.3.

Preparation of bis-(β-ketoamino)nickel(II) complex

Bis-(β-ketoamino)nickel(II) complexes Ni[R1C(O)CHC(NR3) R2]$_2$ (Scheme 1), which were here employed to act as catalysts precursors for polymerization of methyl methacrylate after activation with MAO, were synthesized according to the preparation method for complexes **5** and **6** reported in our previous work.[14] Complexes **1–6** were prepared using a two-step procedure. The first step consisted of a condensation reaction between a β-diketo compound and one equivalent of an aromatic amine to afford the respective β-ketoamine ligands. These were subsequently deprotonated using *tert*-BuOK, and finally exposed to the desired nickel for complexation by mixing with $[Et_4N]_2[NiBr_4]$ in *tert*-BuOH solvent.

Crystal structure determination

The crystals were mounted on a glass fiber using the oil drop scan method.[15] Data obtained with the $\omega-2\theta$ scan mode were collected on a Bruker SMART 1000 CCD diffractometer with graphite-monochromated Mo-K_α radiation ($\lambda = 0.71073$ Å) at 293 K. The structures were solved using direct methods, while further refinement with full-matrix least squares on F^2 was obtained with the SHELXTL program package.[16,17] All nonhydrogen atoms were refined anisotropically. Hydrogen atoms were introduced in calculated positions with the displacement factors of the host carbon atoms.

Polymerization of methyl methacrylate

Solution polymerization of methyl methacrylate was carried out in a 50 ml two-necked round-bottomed flask containing a magnetic stir bar and connected with a vacuum system. In a typical procedure, the appropriate MAO solid was first introduced into the round-bottomed glass, then 10 ml toluene and 10 ml of a toluene solution of methyl methacrylate (0.5 g/ml) were syringed into the well-stirred solution in order. Finally, an appropriate amount of fresh Ni(II) catalyst solution (in toluene, 0.005 mol/l) was syringed in to initiate polymerization. The reaction solution was kept well stirred at a constant polymerization temperature under nitrogen. After a given time, polymerizations were stopped by addition of acidic EtOH (5% v/v solution of HCl). The resulting precipitated PMMA was collected and treated by filtering, washing with EtOH several times, and drying in vacuum at 60 °C to a constant weight. Polymer yield was determined by gravimetry. Unless otherwise stated, the total reaction volume was kept at 21 ml, achieved by varying the amount of toluene added if necessary.

Characterization of polymer

The weight-average molecular weights (M_w) and molar mass distributions (M_w/M_n) of the polymers were measured by gel permeation chromatography (GPC) using a Waters 150C instrument operated at 40 °C using chloroform ($CHCl_3$) as the solvent and calibrated using polystyrene standards as the reference. ^1H and ^{13}C NMR spectra were recorded on

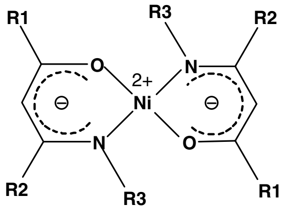

R1	R2	R3	Complex
Me	Me	2,6-diisopropylphenyl	**1**
Ph	Me	2,6-diisopropylphenyl	**2**
Me	Me	Naphthyl	**3**
Ph	Me	Naphthyl	**4**
Me	Me	2,6-dimethylphenyl	**5**
Me	Me	Phenyl	**6**

Scheme 1.

an INOVA 500 Hz at 120 °C in $o\text{–}C_6H_4Cl_2$ and $o\text{–}C_6D_4Cl_2$ solution (using TMS as the internal reference for ^{1}H NMR); chemical shifts were reported in ‰ ppm downfield from TMS. The triad tacticities of the PMMA microstructure were determined by using the area ratios of α-methyl carbon splitting peaks in ^{13}C NMR spectra. FTIR spectra were recorded on a Nicolet 205 FTIR using conventional KBr pellets method.

RESULTS AND DISCUSSION

Synthesis and structure of bis-(β-ketoamino) nickel(II) complex

Complexes **1**–**6** were prepared using a two-step procedure. The first step consisted of a condensation reaction between a β-diketo compound and one equivalent of an aromatic amine to afford the respective β-ketoamine ligands which were subsequently deprotonated using *tert*-BuOK, and finally exposed to the desired nickel for complexation by mixing with $[Et_4N]_2[NiBr_4]$ in *tert*-BuOH solvent.

Single crystals of nickel complexes **1, 3** and **4** suitable for X-ray structure determination were recrystallized from toluene–hexane (1 : 3, v/v). The ORTEP diagrams are shown in Figs 1–3, respectively. The crystallographic data for complexes **1, 3** and **4** are summarized in Table 1.

As depicted in Figs 1–3, the crystal structures of complexes **1, 3** and **4** are similar to the analogue complexes **5** and **6** we previously reported,[14] and all share the four-coordination binding mode around nickel(II) center.

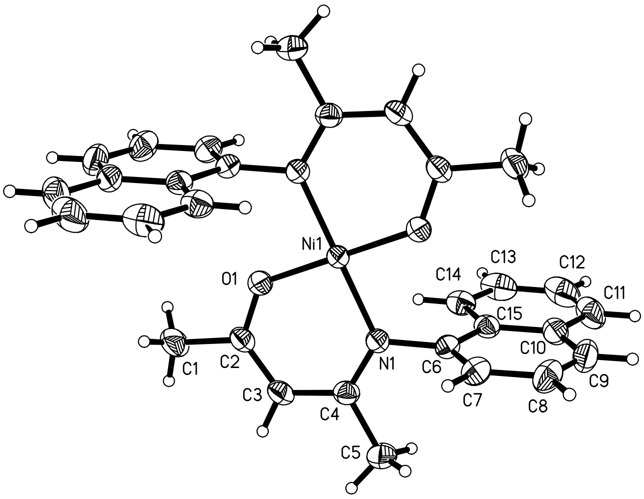

Figure 1. ORTEP plots of complex **1**. Selected bond lengths (Å) and angles (deg): Ni(1)–O(1), 1.8220(12); Ni(1)–N(1), 1.9162(12); C(2)–O(1), 1.280(2); C(4)–N(1), 1.318(2); C(6)–N(1), 1.4342(19); C(1)–C(2), 1.505(2); C(2)–C(3), 1.362(3); C(3)–C(4), 1.398(2); O(1)–Ni(1)–N(1), 92.77(5); O(1)–Ni(1)–O(1)#1, 180.00(9); N(1)#1–Ni(1)–N(1), 180.00(11); O(1)–Ni(1)–N(1)#1, 87.23(5); C(2)–O(1)–Ni(1), 129.15(11); C(6)–N(1)–Ni(1), 117.51(10); C(4)–N(1)–Ni(1), 125.53(11); C(2)–C(3)–C(4), 124.29(15).

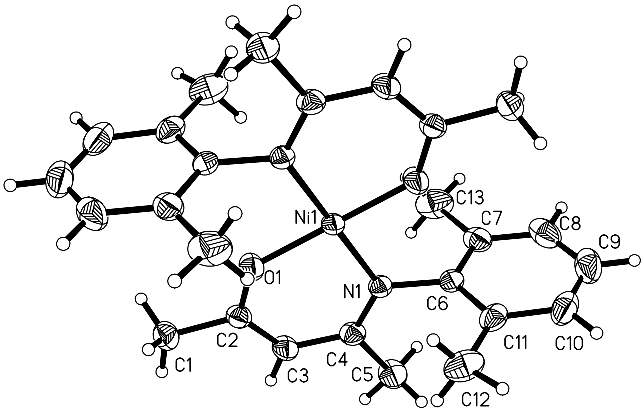

Figure 2. ORTEP plots of complex **3**. Selected bond lengths (Å) and angles (deg): Ni(1)–O(1), 1.8186(13); Ni(1)–N(1), 1.9239(13); C(2)–O(1), 1.279(2); C(4)–N(1), 1.321(2); C(6)–N(1), 1.438(2); C(1)–C(2), 1.500(3); C(2)–C(3), 1.362(3); C(3)–C(4), 1.409(3); C(4)–C(5), 1.513(3); C(7)–C(8), 1.393(3); C(7)–C(13), 1.493(3); O(1)–Ni(1)–N(1), 92.81(6); O(1)–Ni(1)–O(1)#1, 180.0; N(1)#1–Ni(1)–N(1), 180.0; O(1)#1–Ni(1)–N(1), 87.19(6); C(2)–O(1)–Ni(1), 130.10(12); C(6)–N(1)–Ni(1), 117.46(10); N(1)–C(4)–C(5), 120.67(17); C(4)–N(1)–Ni(1), 125.45(12); C(7)–C(6)–N(1), 120.06(17).

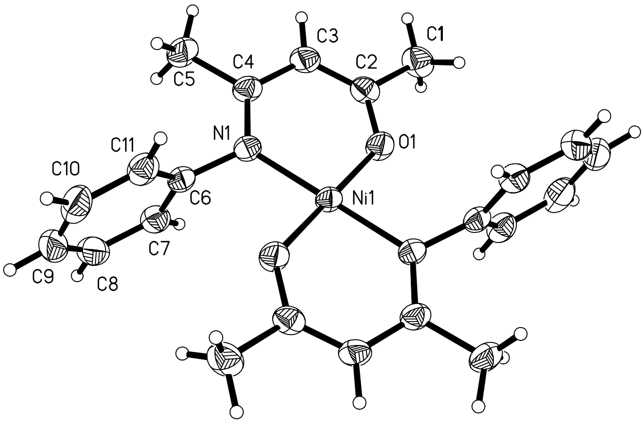

Figure 3. ORTEP plots of complex **4**. Selected bond lengths (Å) and angles (deg): Ni(1)–O(1), 1.8365(12); Ni(1)–N(1), 1.9193(13); C(2)–O(1), 1.285(2); C(4)–N(1), 1.320(2); C(6)–N(1), 1.437(2); C(1)–C(2), 1.508(3); C(2)–C(3), 1.365(3); C(3)–C(4), 1.406(3); C(4)–C(5), 1.512(3); C(6)–C(7), 1.378(3); O(1)–Ni(1)–N(1), 92.37(6); O(1)–Ni(1)–O(1)#1, 180.00(8); N(1)#1–Ni(1)–N(1), 180.00(8); O(1)–Ni(1)–N(1)#1, 87.63(6); C(2)–O(1)–Ni(1), 128.50(12); C(6)–N(1)–Ni(1), 118.05(10); C(4)–N(1)–Ni(1), 125.14(12); C(4)–N(1)–C(6), 116.79(14); N(1)–C(4)–C(5), 120.76(17); N(1)–C(4)–C(3), 122.94(16); C(11)–C(6)–N(1), 121.06(16); C(7)–C(6)–N(1), 121.06(16).

Table 1. Crystallographic data for complexes **1, 3** and **4**

	1	**3**	**4**
Empirical formula	$C_{30}H_{28}N_2NiO_2$	$C_{26}H_{32}N_2NiO_2$	$C_{22}H_{24}N_2NiO_2$
Formula weight	507.25	463.25	407.14
Crystal color and form	Dark green	Dark brown	Dark brown
Crystal system	Triclinic	Monoclinic	Monoclinic
Space group	P-1	P2(1)/c	P2(1)/c
a (Å)	7.4068(9)	10.2883(12)	10.2015(13)
b (Å)	7.8616(10)	10.7074(13)	6.9740(9)
c (Å)	11.5781(14)	14.6761(18)	17.034(2)
α (deg)	99.734(2)	90	90
β (deg)	94.940(2)	130.600(2)	124.729(2)
γ (deg)	107.924(2)	90	90
V (Å^3)	625.33(13)	1227.5(3)	996.0(2)
Z	1	1	2
Dc (mg/m^3)	1.347	1.253	1.358
Absolute coefficient μ (mm^{-1})	0.805	0.814	0.992
F (000)	266	492	428
Crystal size (mm)	0.50 × 0.42 × 0.24	0.50 × 0.35 × 0.30	0.42 × 0.38 × 0.24
θ_{max} (deg)	27.07	27.04	27.02
Index ranges	$-9 \le h \le 9$	$-13 \le h \le 11$	$-8 \le h \le 13$
	$-10 \le k \le 10$	$-10 \le k \le 13$	$-8 \le k \le 8$
	$-14 \le I \le 14$	$-16 \le I \le 18$	$-21 \le I \le 21$
Number of permutations	162	146	126
Goodness-of-fit on S (F^2)	1.117	1.067	1.029
Final R indices [$I > 2\sigma$ (I)]	0.0310; 0.0807	0.0308; 0.0822	0.0282; 0.0763
R indices (all data)	0.0330; 0.0826	0.0415; 0.0915	0.0367; 0.0825
Largest differential peak and hole (e/Å^{-3})	0.365 and −0.171	0.523 and −0.224	0.254 and −0.178

$R = \sum ||F_o|-|F_c|| \sum |F_o|$; $R_w = [\sum_w (F_o^2 - F_c^2)^2 / \sum_w (F_o^2)^2]^{1/2}$.

Effect of polymerization temperature

In order to test the necessity of adding the Ni complexes with MAO for MMA polymerization, blank experiments were first conducted by mixing MMA with either bis(β-ketoamino)nickel(II) or MAO alone or without either bis(β-ketoamino)nickel(II) or MAO at 50 °C for 20 h. It was found that MMA did not polymerize in each case described above. In this study, therefore, binary-component catalysts are necessary to initiate MMA polymerization, and MAO used as a cocatalyst plays an important role in promoting the polymerization of MMA.

Polymerization of MMA with bis-(β-ketoamino)nickel(II) (**1**–**4**) complexes in combination with MAO were carried out at different polymerization temperatures (T_p) with constant ratios of monomer to Ni complex and MAO to Ni complex. The results are summarized in Table 2. All the catalysts showed moderate activities, and the catalytic activities obviously depend on polymerization temperature. The highest activity values were achieved at about 50 °C, but led to a sharp decrease as T_p was increased to 70 °C.

As shown in Table 2, these compounds catalyzed the polymerization of MMA to give high molecular weight polymers with rather broad molecular weight distributions. With increasing T_p, the molecular weights of the polymers increase and with polydispersities similar to the results obtained with the Ni(acac)$_2$–MAO catalyst reported by Coutinho *et al.*[18] Interestingly, the polydispersity value broadens continuously as T_p increases; the reason for this phenomenon is not clear. We suggest that the MMA polymerization mechanism may be accompanied by other polymerization mechanisms at higher polymerization temperatures.

Making a comparison between the catalyst features of these Ni complexes for MMA polymerization at 50 °C (see Table 2), the catalytic activity sequence was found to be **4** > **1** > **2** > **3** > **5** > **6**. This is contrary to the expected steric effects of the ketoamino ligand, which are in the order **6** > **5** > **3** > **2** > **1** > **4**. It is evident that steric bulk has an effect on the activities. Smaller substituents on the imino group favor higher catalytic activity. Among these nickel β-ketoamine catalysts, catalyst **4** with phenyl on the imino group exhibited the highest activity, and catalyst **6** with 2,6-diisopropyl phenyl substituents on the imino group showed the lowest activity.

Table 2. Influence of the reaction temperature on the polymerization of MMA catalyzed by **1**–**4**–MAO systems[a]

Run	Catalyst	T_p (°C)[b]	Yield (%)	Activity[c]	M_w (g/mol)[d]	M_w/M_n[d]
1	**1**	0	trace	0	nd	nd
2	**1**	25	6.52	6.52×10^4	0.67×10^5	2.89
3	**1**	50	22.9	2.29×10^5	0.94×10^5	3.76
4	**1**	70	16.3	1.63×10^5	1.33×10^5	5.21
5	**2**	0	3.38	3.38×10^4	0.49×10^5	2.56
6	**2**	25	9.30	9.30×10^4	0.88×10^5	4.61
7	**2**	50	20.4	2.04×10^5	1.66×10^5	5.96
8	**2**	70	9.10	9.10×10^4	1.84×10^5	6.12
9	**3**	0	trace	0	nd	nd
10	**3**	25	trace	0	nd	nd
11	**3**	50	17.7	3.54×10^4	0.99×10^5	3.01
12	**3**	70	14.9	2.99×10^4	1.25×10^5	4.68
13	**4**	0	trace	0	nd	nd
14	**4**	25	0.99	9.90×10^3	1.07×10^5	3.98
15	**4**	50	37.7	3.77×10^5	1.58×10^5	5.02
16	**4**	70	24.3	2.43×10^5	1.87×10^5	6.11
17	**5**[e]	0	0.84	1.20×10^3	0.38×10^5	2.30
18	**5**[e]	25	1.72	3.59×10^3	0.65×10^5	2.60
19	**5**[e]	50	13.0	1.86×10^4	0.83×10^5	4.34
20	**5**[e]	70	2.30	9.54×10^3	1.45×10^5	6.01
21	**6**[e]	0	0.50	0.75×10^3	0.42×10^5	2.46
22	**6**[e]	25	0.93	1.33×10^3	0.60×10^5	2.93
23	**6**[e]	50	5.40	7.65×10^3	0.74×10^5	5.64
24	**6**[e]	70	3.40	4.89×10^3	1.54×10^5	6.07

[a] Polymerization conditions: Ni = 5×10^{-3}mmol; MMA = 0.05mol; [Al]:[Ni] = 600; t_p = 1 h (for **1** and **2**); [Al]:[Ni] = 600; t_p = 5 h (for **3**); [Al]:[Ni] = 620; t_p = 1 h (for **4**).

[b] Polymerization temperature. [c] Activity in gPMMA (mol Ni h)$^{-1}$. [d] Solvent: chloroform; temperature: 40 °C; M_w are the relative weight-average molecular weight, and calibration with polystyrene standards.

[e] The polymerization results catalyzed by **5** and **6**– MAO:[14] t_p = 7 h; [Al][Ni] = 945; n.d.: not determined.

Effect of Al : Ni ratio

For binary catalysts, the ratio of both catalyst components will influence the polymerization activity. As shown in Fig. 4, the polymer yields increase sharply with increases in the Al : Ni ratio up to 700, but further increases in the Al/Ni molar ratio lead to lower yields. As for the catalytic activity, the optimum Al : Ni molar ratio range is 600–900.

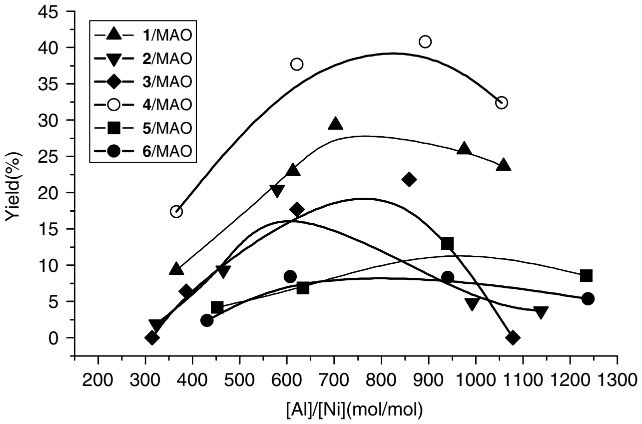

Figure 4. Influence of [Al]:[Ni] ratios on the yields of polymerization of MMA catalyzed by (**1**–**6**)–MAO systems at 50 °C.

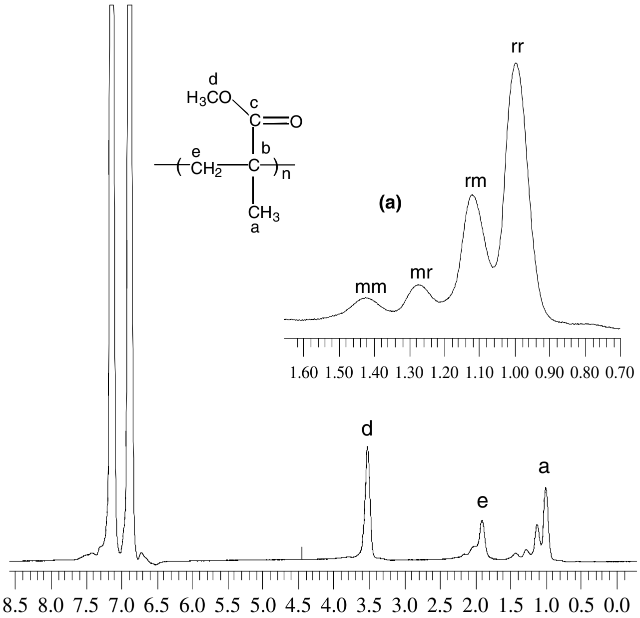

Figure 5. ^1H NMR spectrum of PMMA in o-$C_6H_4Cl_2$ and o-$C_6D_4Cl_2$ at 120 °C obtained by **1**–MAO system at 50 °C.

^{1}H and ^{13}C NMR spectra of polymer

Figures 5 and 6 show typical ^1H and ^{13}C NMR spectra for PMMA obtained from the **1**–MAO catalyst system at 50 °C and determined at 120 °C in o–$C_6H_4Cl_2$. As seen in Fig. 5, in the 0.8–3.8 ppm range, three groups of hydrogen protons appear, which are assigned to the hydrogen protons of α-methyl(H_a), methoxy(H_d) and methenes(H_e) in the MMA units, respectively. The ^{13}C NMR spectrum also shows the characteristic chemical-shift signals of the carbon types in MMA units. The chemical-shift signals appearing around 175.79–177.84 ppm (c), 18.25–22.24 ppm (a), 52.78–54.63 ppm (e), 49.52–51.37 ppm (d) and 43.73–45.60 ppm (b) can be assigned to the resonances of ester carbonyl (C=O), α-methyl (α–CH_3), methoxy (–OCH_3), methenes (–CH_2–) and quaternary carbons in MMA units, respectively.

The triad tacticities were determined by using the area ratios of α-methyl(α–CH_3) carbon splitting peak in ^{13}C NMR spectra, and the resulting analyses of rr, mr, mm stereo-triad distributions obtained using the bis(β-ketoamino)nickel(II)(**1**–**6**)–MAO catalytic system at 50 °C are

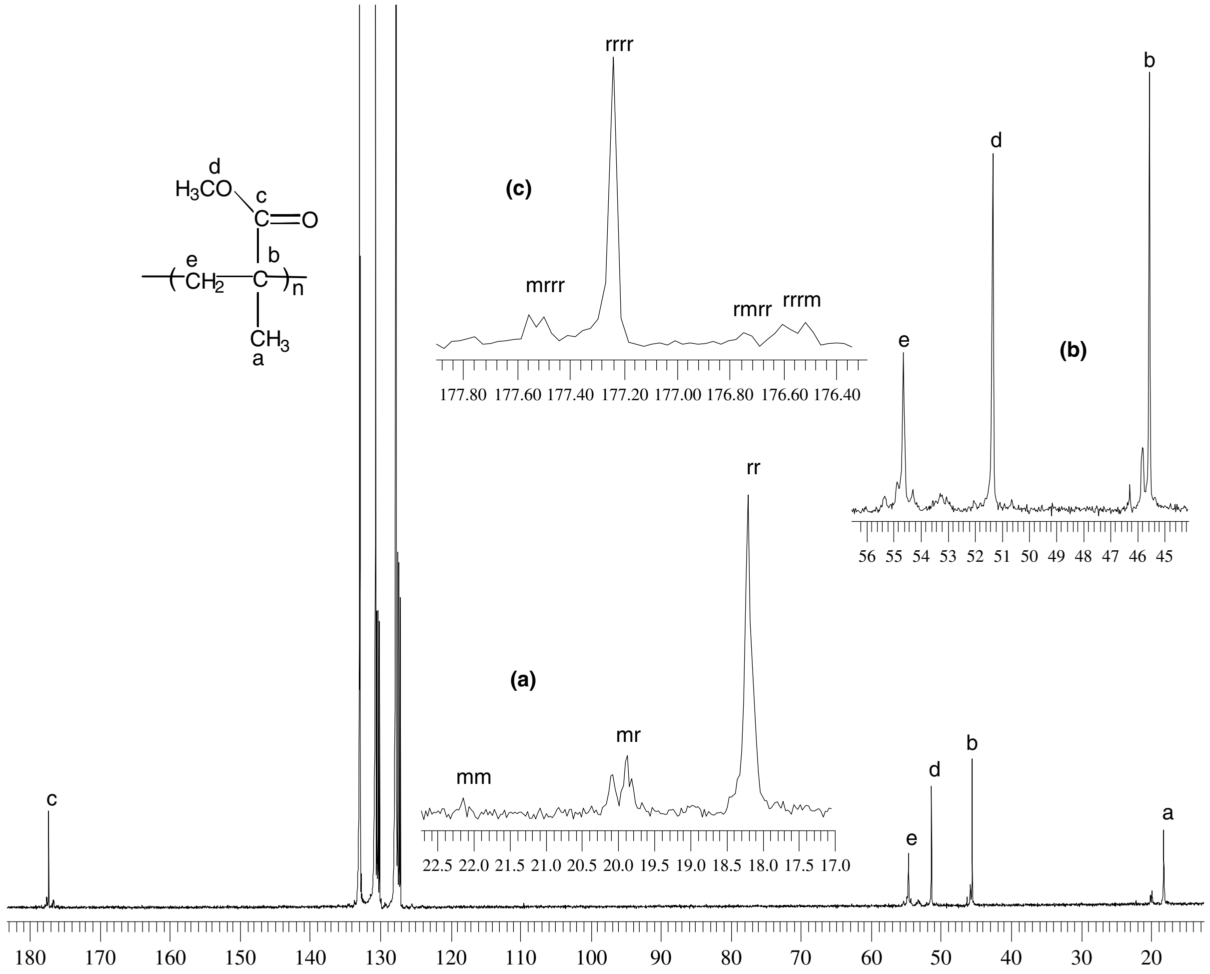

Figure 6. ^{13}C NMR spectrum of PMMA in o-$C_6H_4Cl_2$ and o-$C_6D_4Cl_2$ at 120 °C obtained by **1**–MAO system at 50 °C.

Table 3. α-Methyl triad tacticity of PMMA obtained with (**1**–**6**)–MAO catalysts in toluene at 50 °C[a]

Catalyst	Triad (mm)	Fractions[b] (mr)	(%) (rr)	Triad A^c	Tests B^c	P (r/m)	P (m/r)	Sum,[d] P(r/m)+ P(m/r)	L (m)	L (r)
1	4.1	29.2	66.7	0.28	1.28	0.781	0.180	0.960	1.281	5.568
2	3.8	34.6	61.6	0.23	0.81	0.814	0.219	1.033	1.229	4.564
3	0.4	33.8	65.8	0.02	0.09	0.977	0.204	1.181	1.024	4.893
4	2.3	33.3	64.4	0.14	0.53	0.879	0.205	1.084	1.138	4.868
5	6.5	33.8	59.7	0.38	1.36	0.722	0.221	0.943	1.385	4.533
6	2.7	31.3	66.0	0.17	0.73	0.853	0.192	1.045	1.173	5.217

[a] [MMA] = 0.05 mol, [Ni] = 5×10^{-3} mmol; $T_p = 50\,°C$; $t_p = 1$ h (for **1, 2** and **4**); $t_p = 5$ h (for **3**); $t_p = 7$ h (for **5** and **6**).
[b] Observed in ^{13}C NMR spectra of α-methyl carbon resonance; from low to high field in the spectra ($\delta = 23.0$–18.0 ppm).
[c] $A = 2(mm)/(mr) = 1$ for site control mechanism and $B = 4(mm)(rr)/(mr)^2 = 1$ for chain-end control mechanism.[19]
[d] If stereoregulation follows a Bernoullian distribution, $P(r/m) + P(m/r) = 1$.[20]

listed in Table 3. All the above catalyst systems produced PMMAs with similar microstructures, and the analyses of the rr, mr, mm stereo-triad distributions indicate that these catalytic systems initiate MMA polymerization to yield PMMA with syndiotactic-rich atactic microstructures (rr content is between 59 and 67%). The variation of substituents on the ligand imino group has little influence on the syndiotacticity (as rr triad) of PMMA. The similarity in polymer microstructures suggests that chain initiation and chain growth most likely proceed along similar pathways for all bis(β-ketoamino)nickel(II)/MAO catalyst systems used in this study.

Study of the mechanism

Based on the proposed mechanism for acrylate polymerization catalyzed by neutral palladium complex $[Pd(C_6F_5)Br(NCMe)_2]$, reported by Sen,[21] and neutral palladium complex $[Pd_2(\mu\text{-}X)_2(C_6F_5)_2L_2]$ [L = tetrahydrothiophene (tht), X = Cl], reported by Espinet,[22] together with the result that distributions of rr, mr and mm stereo-triads of the poly(methyl methacrylate) in this study had a syndio-rich atactic microstructure similar to that of PMMA prepared with a free radical initiator,[23–25] we can suggest that the polymerization of MMA with bis(β-ketoamino)nickel(II)–MAO catalyst runs using a similar radical polymerization mechanism (as shown in Scheme 2).

The first step involves the 2,1-type insertion of methyl methacrylate into the Ni–R bond to form stable alkyl complexes that act as a kind of reservoir of radical species and of Ni–H, providing a slow but steady supply of catalytically active species. In the second step the nickel–carbon bond of the alkyl complex homolyzes and generates radicals. The radicals initiate further polymerization and bring about polymer growth and MMA will form new radicals by successive addition of methyl methacrylate monomer to the alkyl radical. The growing radical chain is in equilibrium with the corresponding nickel-bound polymeric alkyl. The third step is that the growing radical will recombine with [Ni] and then follow chain termination by β-H elimination occurring from the β-H elimination of the methyl group and the methylene group in MMA because of its facility. The fast formation of nickel hydride produces a high concentration of

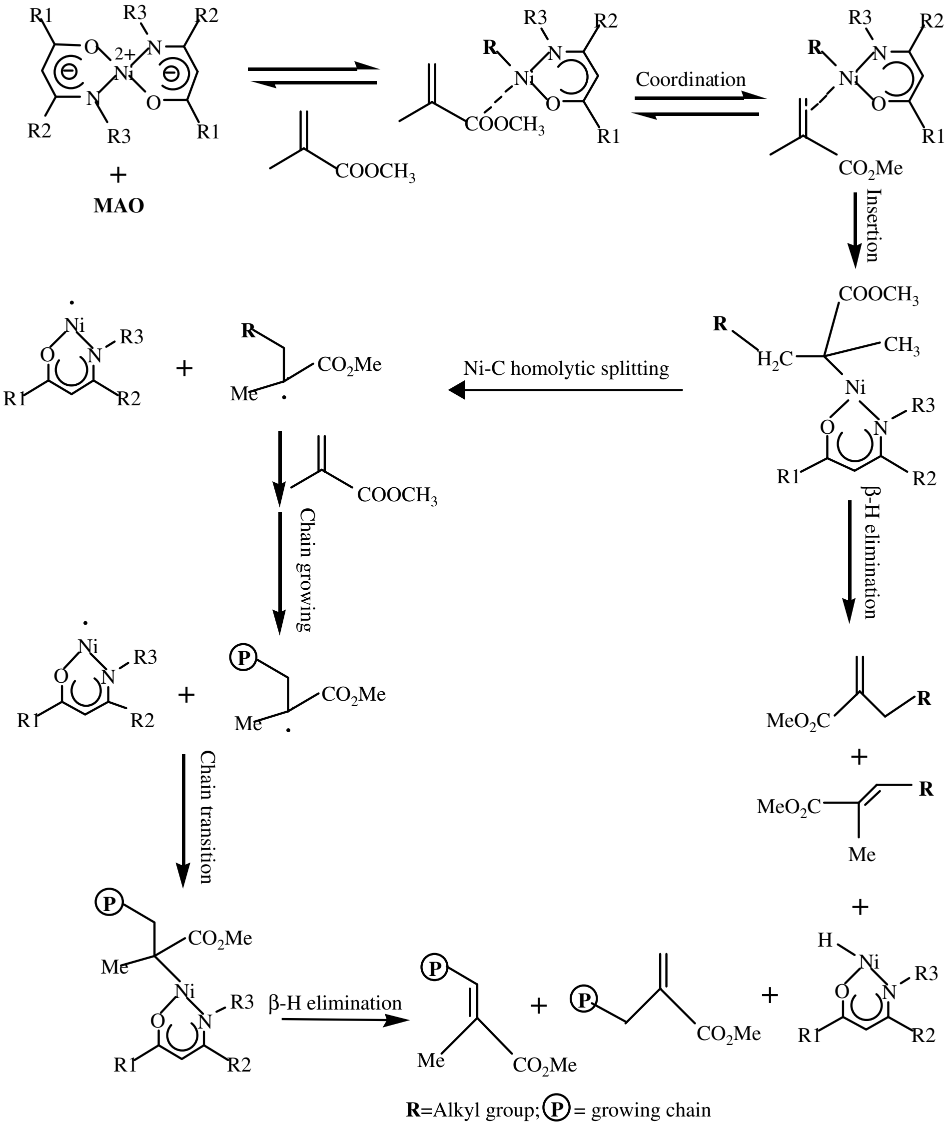

Scheme 2. Proposed mechanism of MMA polymerization catalyzed by bis(β-ketoamino)nickel(II)–MAO system.

hydride species and leads to its immediate decomposition, and the initiator is consumed irreversibly in the stages of the reaction, in addition. It is worth noting that nickel–carbon bond homolysis can compete with the insertion of methyl methacrylate into the Ni–H bond, but it is reversible and, at any given time, the concentration of radicals is low.

CONCLUSIONS

We have synthesized a series of new bis(β-ketoamino) nickel(II) complexes and examined their catalytic behavior for the polymerization of MMA. All these nickel complexes can act as catalyst precursors after activation with MAO for polymerization of MMA with moderate activities, and produce PMMA with a syndiotactic-rich atactic microstructure with wide polydispersity ($M_w/M_n > 2$). Distributions of rr, mr and mm stereo-triads of the polymers were examined by NMR. $P(\mathrm{r/m}) + P(\mathrm{m/r})$ is approximately 1, indicating that the microtacticity distributions of PMMA can be considered to obey Bernoullian statistics. Based on the literature and the result in this study, a radical polymerization mechanism has been proposed for MMA polymerization with the bis(β-ketoamino)nickel(II)–MAO catalyst system.

Acknowledgements

The support from the NSFC and SINOPEC (joint-project 20334030), the Science Foundation of Guangdong Province (project 039184) and the Ministry of Education of China (20030558017) are gratefully acknowledged.

Supporting information available

CIF data of **1, 3** and **4** are available free of charge at: http://pubs.acs.org.

REFERENCES

1. Lisa SB, Novak BM. *Chem. Rev.* 2000; **100**: 1479.
2. Yasuda H, Ihara E. *Adv. Polym. Sci.* 1997; **133**: 53.
3. Yasuda H. *Macromol. Chem. Phys.* 1995; **196**: 2417.
4. Deng H, Shiono T, Soga K. *Macromolecules* 1995; **28**: 3067.
5. Nakayama Y, Shibahara T, Hukumoto H, Nakamura A, Mashima K. *Macromolecules* 1996; **29**: 8014.
6. Ittel SD, Johnson LK, Brookhart M. *Chem. Rev.* 2000; **100**: 1169.
7. Soga K, Deng H, Yano T, Shiono T. *Macromolecules* 1994; **27**: 7938.
8. Deng H, Shiono T, Soga K. *Macromol. Chem. Phys.* 1995; **196**: 1971.
9. Deng H, Shiono T, Soga K. *Macromolecules* 1995; **28**: 3067.
10. Shiono T, Saito T, Saegusa N, Hagihara H, Ikeda T, Deng H, Soga K. *Macromol. Chem. Phys.* 1998; **199**: 1573.
11. Cameron PA, Gibson VC, Graham AJ. *Macromolecules* 2000; **33**: 4329.
12. Kim I, Hwang JM, Lee JK, Ha CS, Woo SI. *Macromol. Rapid Commun.* 2003; **24**: 508.
13. Kim I, Kim JS, Han BH, Ha CS. *Macromol. Res.* 2003; **11**: 514.
14. He X, Yao Y, Luo X, Zhang J, Liu Y, Zhang L, Wu Q. *Organometallics* 2003; **22**: 4952.
15. Kottke T, Stalke D. *J. Appl. Crystallogr.* 1993; **26**: 615.
16. *SHELXTL*, Version 5.1. Bruker AXS: Madison, WI, 1998.
17. Sheldrick GM. *SHELXL-97*, program for X-ray Crystal Structure Solution and Refinement. Göttingen University: Göttingen, 1998.
18. Coutinho FMB, Costa MAS, Monteiro LF, Maria LC. *Polym. Bull.* 1997; **38**: 303.
19. Konishi T, Tamai Y, Fujii M, Einaga Y, Yamakawa H. *Polym. J.* 1989; **21**: 329.
20. Hatada K, Kitayama T, Ute K. *Polym. Sci.* 1988; **13**(4): 189.
21. Elia C, Sharon EB, Sen A, Raquel LF, Albeniz AC, Espinet P. *Organometallics* 2002; **21**: 4249.
22. Albeniz AC, Espinet P, Raquel LF. *Organometallics* 2003; **22**: 4206.
23. Bovey FA, Jelinski LW. *Chain Structure and Conformation of Macromolecules.* Academic Press: New York, 1982; 48.
24. Bovey FA, Tiers GVD. *J. Polym. Sci.* 1960; **44**: 173.
25. Frisch HL, Mallows CL, Heatley F, Bovey FA. *Macromolecules* 1968; **1**: 533.